1-1-2005

Deformation behaviour of a new type AL-MG-SI-CU alloy

Lizi He

A. K. Tieu
University of Wollongong, ktieu@uow.edu.au

Cheng Lu
University of Wollongong, chenglu@uow.edu.au

Yanbo Chen

Hongtao Zhu
University of Wollongong, hongtao@uow.edu.au

DEFORMATION BEHAVIOR OF A NEW TYPE AL-MG-SI-CU ALLOY

L.Z. He[a, b], A.K. Tieu[a], C. Lu[a], Y.B. Chen[a,b], H.T. Zhu[a]
[a] School of Mechanical, Materials and Mechatronics, University of Wollongong, Wollongong, NSW 2522, Australia; [b] School of Materials and Metallurgy, Metal Forming, Northeastern University, Shenyang 110004, China

Summary

The deformation behavior of Al-1.01Mg-0.68Si-1.78Cu alloy at various heat treatment conditions has been investigated. The effect of ageing treatment, transition elements and grain boundary on the deformation behavior is also discussed. The detailed fracture surfaces and dislocation structures are examined through scanning electron microscopy (SEM) and transmission electron microscopy (TEM). The results show that the tensile properties, deformation and fracture behavior are closely related to the ageing conditions.

Keywords: Al-Mg-Si-Cu alloy, deformation behavior, ageing treatment

1 Introduction

Al-Mg-Si alloys are medium strength heat-treatable wrought alloys possessing a wide range of mechanical properties, good workability, weldability and corrosion resistance. They are widely used as structural and architectural materials. Several research works have been undertaken to strengthen the alloys either by a small copper addition [1-5] or by a pre-deformation treatment [6-10]. The copper addition increases the peak hardness and yield strength during artificial ageing. Some studies showed that the strengthening due to copper addition was caused by the additional precipitation of S', θ' and Q phases [5, 11-13].
The potential for increased use of the new 6000 series alloys in the demanding environment of the aerospace industry, however, has created the desire for a more insight into the microstructure and mechanical properties of the alloys. The present investigation is carried out to study the deformation behavior of Al-1.01Mg-0.68Si-1.78Cu alloy at various ageing conditions, and the fracture behavior is also discussed.

2 Experimental procedures

The composition of semi-continuous cast alloy used in this work is given in Table 1. The alloy was prepared using 99.97% commercial pure aluminum, 99.99% copper, 99.99% magnesium as well as master alloys of Al-20wt.%Si, Al-10wt.%Mn, Al-2.5wt.%Cr, Al-

5wt.%Ti, Al-4wt.%Zr. The size of ingot is 200×1300×30mm. The as-cast ingots were homogenized at 520^{0}C for 12 hours and followed by air cooling. After hot rolled by 85% at 450^{0}C, the ingots were annealed at 415^{0}C for 2-3 hours and followed by furnace cooling, and then cold rolled to 1.5mm by 65%. The solution treatment was performed in a salt bath ($NaNO_3/KNO_3$=1) at 540^{0}C for 20 minutes, and then quenched in cold water to room temperature. Artificial ageing was conducted in a salt bath ($NaNO_2/KNO_2$=1) at 170^{0}C for various times to get the underaged (UA), peaking aged (PA) and overaged (OA) conditions. The temperature was maintained within ±1^{0}C during ageing treatment.

Table1: The composition of the test alloy (wt.%)

Cu	Mg	Si	Cr	Mn	Ni	Zn	Fe
1.78	1.01	0.68	0.19	<0.05	<0.01	<0.05	0.15

Sample for tensile tests of 10×1mm gage transverse section and of 50mm gage length were machined from the artificial aged sheets. Tensile tests were carried out on an Instron 1123 at room temperature in air, with a crosshead speed of 10mm/min. The microstructure observations were made on a Philip EM420 type transmission electron microscopy (TEM). Thin foils were prepared by twin-jet thinning electrolytically in a solution of 30% nitric acid and 70% methanol at -25^{0}C. Tensile fracture surface examinations were performed on a Cambridge S360 scanning electron microscopy (SEM).

3 Results and discussion

The tensile properties of the test alloy aged at 170^{0}C for different times are shown in Figure 1. Both the ultimate tensile strength (UTS) and yield strength (YS) increase sharply at the early stage of the ageing treatment, reach the peak value of UTS= 435MPa and YS=359 MPa at 7h. After that point, the UTS and YS decrease slightly up to 12h and then increase again. They reach the second peak value of UTS=438MPa and YS=361MPa at 18h, and change little afterwards. The elongation decreases significantly and reaches the minimum value of 11.6%.
Figure 2 shows the typical tensile stress-strain curves of the alloy under different ageing conditions. It can be seen that the yield stage of quenched alloy is the longest. The ageing treatment shortens the yield stage significantly, especially after the ageing time exceeds 7h. The strain hardening exponent (n) and the uniform elongation change with ageing time are illustrated in Figure 3. Both the n value and the uniform elongation decrease intensively and reach the saturated value at 7h of 0.16 and 9.5%, respectively.
The typical microstructures under different ageing conditions are displayed in Figure 4. In the UA alloy (Fig.4a), profuse plenty of extremely fine particles about a few nanometers (the black dots) precipitate homogeneously in the Al matrix. The appearance of the precipitates is in agreement with the observations for the Guinier-Preston (GP) zones [14, 15]. A large amount of needle-shaped precipitates clearly delineated by strain-field contrast are present in the PA alloy (Fig.4b), parallel to the [100] and [010] matrix directions, identified as the β" phase [15]. The OA alloy (Fig.4c) exhibits a homogeneous distribution of the lath-shaped β'

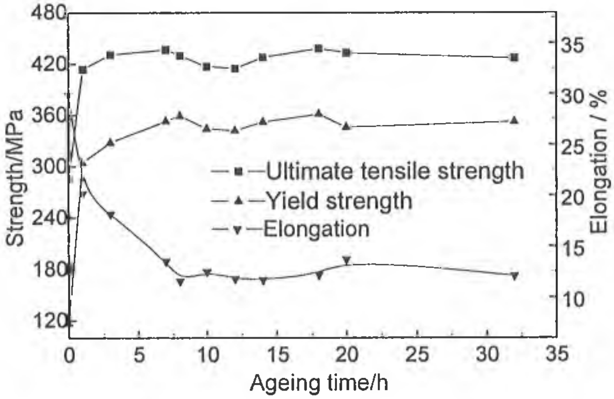

Figure 1: *The effect of ageing conditions on tensile properties of the test alloy aged at 170^{0}C*

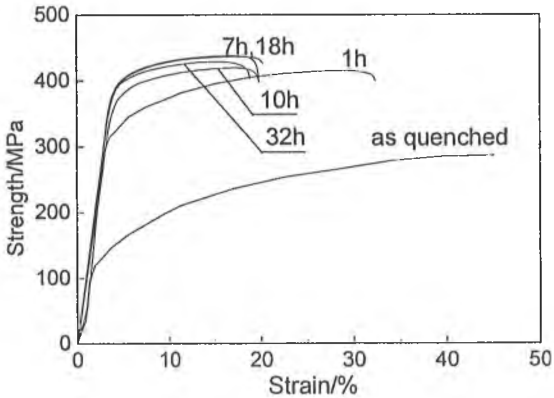

Figure 2: *Typical tensile stress-strain curves of the alloy under different ageing conditions*

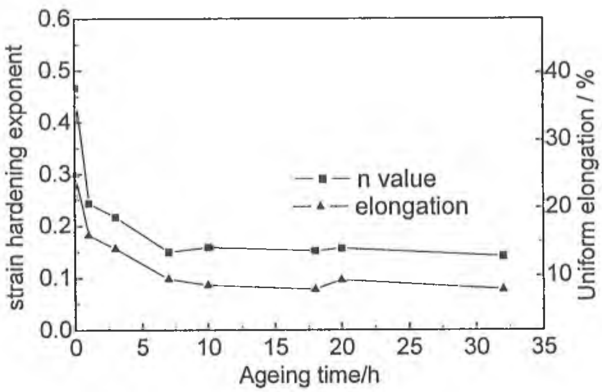

Figure 3: *The effect of ageing conditions on n value and uniform elongation of the alloy*

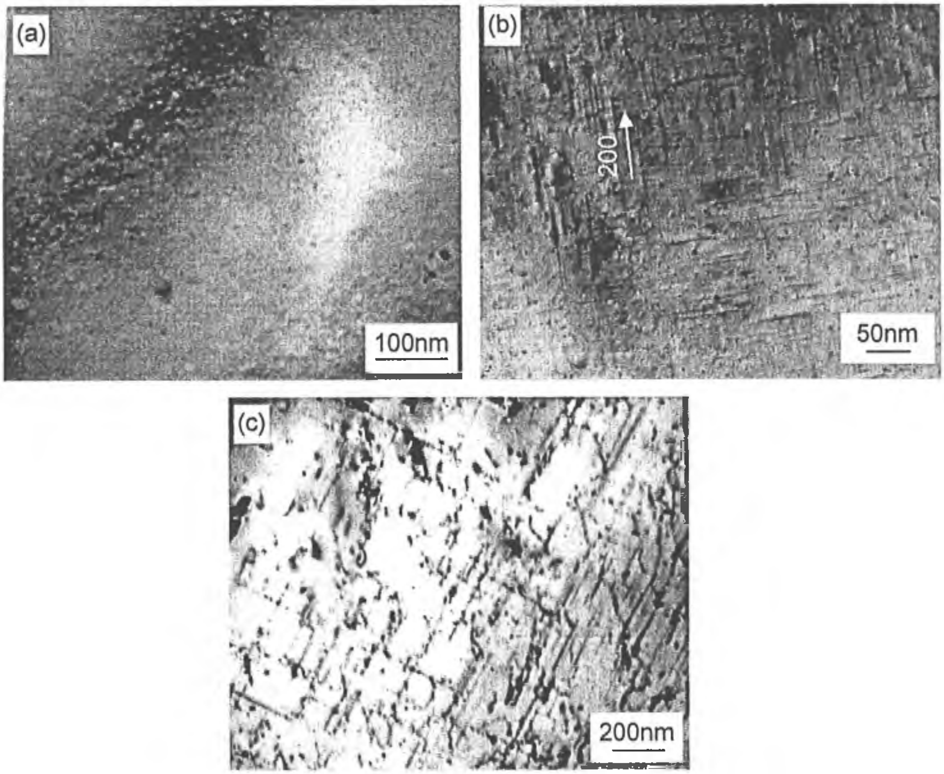

Figure 4: *TEM micrographs showing (a) the GP zone in the UA state (170^{0}C for 1h); (b) the β'' precipitates in the PA condition (170^{0}C for 7h), as thin needles along the [100] and [010] directions of Al matrix; (c) the β' rod-shaped precipitates in the OA state (170^{0}C for32h).*

precipitates, which become larger and often show many dislocations in the region close to the interface.

Figure 5 shows the dislocation structures of the alloy under different ageing conditions after tensile tests. High density tangled dislocations homogeneously distribute in the Al matrix under UA condition (Fig.5a). In PA alloy (Fig.5b), the deformation is still uniform, but the slip bands which contain many tangled dislocations can be found at local regions (as shown by arrows). The dark particles of Fe-bearing phases are also observed in the alloy. In OA alloy (Fig.5c), the deformation is very inhomogeneous and mainly localized in slip bands.

The effect of the ageing conditions on the fracture mode of the alloy is shown in Figure 6. The microstructure contains large amount of dimples on the fracture surface of the UA alloy (Fig.6a). Fracture follows a transgranular path and is entirely ductile. In the PA alloy (Fig.6b), many dimples are also found, but the characteristics of intergranular fracture can be seen in local region, as shown by arrow. In the OA alloy (Fig.6c), the intergranular fracture becomes the main mode.

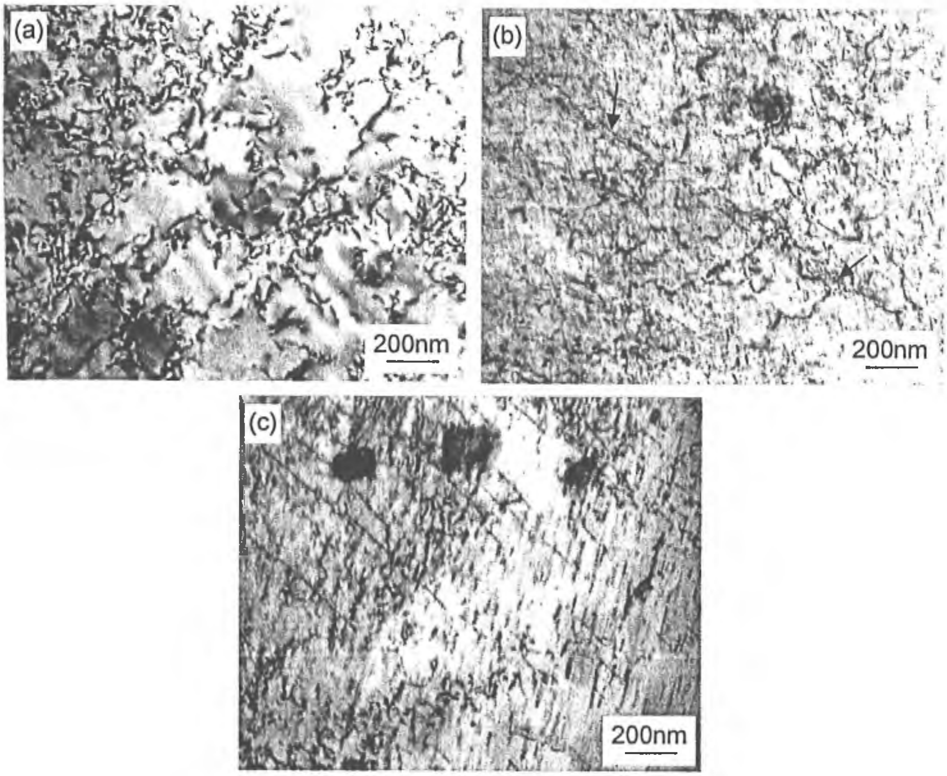

Figure 5: *TEM micrographs showing (a) and (b) localized dislocations and many slip bands in UA alloy (170^0C for 1h) and in PA alloy (170^0C for 7h), respectively; (c) dislocation by-pass larger β' precipitates in OA alloy (170^0C for32h).*

From the above observations, it can be seen that the deformation behavior is controlled by the interaction of dislocations and precipitates for the alloy, and is closely related to the ageing conditions.

For 6000-series alloys, heat treatment is used to promote the formation of needle-shaped precipitates from the supersaturated solid solution of Mg and Si in Al to achieve appreciable mechanical properties. Some extremely fine (about 1-2nm) spherical GP zones precipitate at the early ageing stage. However, considerable confusion remains concerning the initial "clustering" processes. Dutta and Allen [16] proposed that GP zone in 6061 alloy is the clustering of Si atoms. It is more plausible that GP zone is the co-clusters that contain Mg and Si atoms [17]. In Al-Si alloys it is thought that Si-atoms accompany vacancies as they condense during and immediately after quenching and it is likely that this process also occurs in Al-Mg-Si alloys, and then Mg atoms move to clusters of Si-atoms. According to the results of tensile tests, the GP zone has certain strengthening effect on the alloy, does not have its own characteristic structure, only involves ordering processes. So homogeneous deformation is observed and the fracture mode is entirely ductil full of dimples in OA alloy. The type of precipitate that gives rise to the maximum strength of the test alloy under the PA condition is

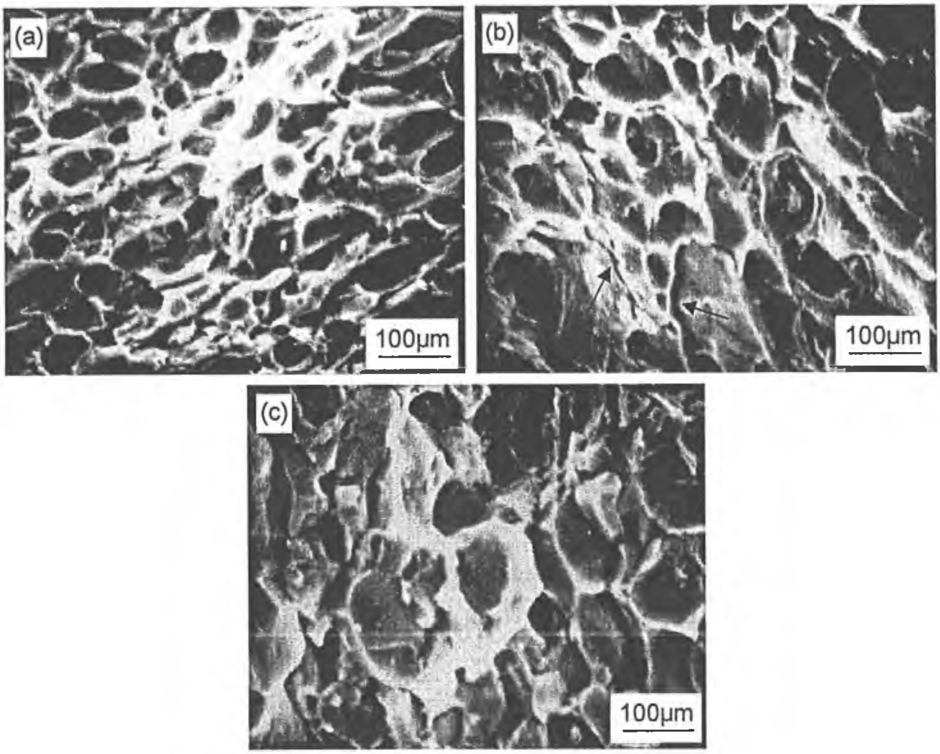

Figure 6: SEM micrographs showing the fracture surfaces of (a) UA alloy (170^{0}C for 1h), (b) PA alloy (170^{0}C for 7h) and (c) OA alloy (170^{0}C for32h) after tensile tests.

β". These precipitates are fine needles, 70nm long, lying parallel to the <001> directions of the matrix. Various crystal structures have been proposed for the β" precipitate: monoclinic with a=c=6.16Å, b=7.1Å and β=82° [18]; monoclinic with a=3.0Å, b=3.3Å, c=4.0Å, γ=71° [18]; hexagonal with a=7.05Å and c=4.05Å [19]. The β" phase are easily cut by moving dislocations leading to an effective softening of slip planes, which promotes heterogeneous deformation and produces planar slip bands. An intergranular fracture characteristic is observed in PA alloy can be attributed to strain localization by particle shearing. Dislocation pileups, arising from such localization, are stopped at grain boundaries or at large particles, a crack nucleates when the critical interfacial strength is locally reached [20]. When the alloy is over-aged, β" precipitates are dissolved and a number of coarser precipitates β' form. The size of β' is still small, so the strength of OA alloy decreases slightly. The β' phase is partly coherent with Al matrix, some dislocations are often observed nearby the β' interface (Fig.4c), During deformation, the stress concentration is high at the region near β', which results in more easily cut by dislocations. Thus, the significant intergranular fracture is found in OA alloy.

4 Conclusion

The spherical GP zone is the main precipitate in UA alloy, tangled dislocations homogeneously distributed in Al matrix, and transgranular fracture is observed.
The needle-shaped β'' precipitates in PA alloy, slip bands shearing β'' are found at local region, and the fracture are partly intergranular.
The coarser needle shaped β' have been observed seen in OA alloy. The deformation is in a highly localized way, with strain concentration attributed to precipitates shearing by dislocation pileups. Fracture is mostly intergranular.

References

[1] Thanaboonsombut, B. and Sanders, T.H.: The Effect of Cooling Rate from the Melt on the Recrystallization Behavior of Aluminum Alloy 6013, Metall. Mater. Trans. A, Vol. 28, No.10(1997), 2137-2142.
[2] Uchida, H., Yoshida, H., Hira, H. and Amano, T.: Development of High Strength Al-Mg-Si-Cu Alloy with Corrosion Resistance, Mater. Sci. Forum, Vol. 217-222(1996), 1753-1758.
[3] Bergsma, S.C. and Kassner, M.E.: The New Aluminum Alloy AA 6069, Mater. Sci. Forum, Vol. 217-222(1996), 1801-1806.
[4] Moons, T., Ratchev, P., De Smeet, P., Verlinden, B. and Van Houtte, P.: A Comparative Study of Two Al-Mg-Si Alloys for Automotive Applications, Scripta Mater., Vol. 35, No.8(1996), 939-945.
[5] Eskin, D.G.: Investigations on the Optimization of Phase and Alloy Compositions of Al-Cu-Si-Mg Alloys, Z. Metallkd., Vol.83, No.10(1992), 762-765.
[6] Burger, G., Gupta, A.K., Sutak, L. and Lloyd D.J.: Recrystallization in a 6000-Series Automotive Sheet Alloy during Solution Heat Treatment Practice, Mater. Sci. Forum, Vol.217-222(1996), 471-477.
[7] Birol, Y.: Pre-straining to improve the bake hardening response of a twin-roll cast Al-Mg-Si alloy, Scripta Mater., Vol. 52, No.3(2005), 169-173.
[8] Zhen, L. and Kang, S.B.: Effect of Predeformation on Microstructure and Tensile Properties of Al-Mg-Si alloys with High Silicon Content, Mater. Sci. Technol., Vol. 14, No.4(1998), 317-321.
[9] Ismail, Z.H.: Microstructure and Mechanical Properties Developed by Thermomechanical Treatment in an AlMgSi Alloy, Scripta Metal. Mater., Vol. 32, No.3(1995), 457-462.
[10] Kwon, Y.N., Lee, Y.S. and Lee, J.H.: Thermomechanical Behavior of Al-Mg-Si Alloys at the Elevated Temperature, Mater. Sci. Forum, Vol. 449-4(2004), 581-584.
[11] Matsuda, K., Kawabata, T., Uetani, Y. and Ikeno, S.: Effect of Addition of Cu on Structures of Metastable Phases in Al-Mg-Si Alloys, Mater. Sci. Forum, Vol. 426-4(2003), 375-380.
[12] Chakrabarti D.J. and Laughlin D.E.: Phase Relations and Precipitation in Al-Mg-Si Alloys with Cu Additions, Progress in Mater. Sci., Vol. 49, No.3-4(2004), 389-410.
[13] Esmaeili, S., Wang, X., Lloyd, D.J. and Poole, W.J.: On the Precipitation-Hardening

Behavior of the Al-Mg-Si-Cu, Metall. Mater. Trans. A, Vol. 34, No.3(2003), 751-763.
[14] Zhen, L., Fei, W.D., Kang, S.B. and Kim, H.W.: Precipitation Behavior of Al-Mg-Si Alloys with High Silicon Content, J. Mater. Sci., Vol. 32(1997), 1895-1902.
[15] Lynch, J.P., Brown, L.M. and Jacobs, M.H.: Microanalysis of Age-Hardening Precipitates in Aluminum Alloys, Acta Metall., Vol. 30, No.7(1982), 1389-1395.
[16] Nutta, I. and Allen, S.M.: A Calorimetric Study of Precipitation in Commercial Aluminum Alloy-6061, J. Mater. Sci. Lett., Vol. 10, No.6(1991), 323-326.
[17] Chatterjee, D.K. and Entwhistle, K.M.: Study of Effect of Magnesium Loss and of Addition of Copper on aging of Aluminum-Magnesium-Silicon Alloys, J. Inst. Metals, Vol. 101(1973), 53-59.
[18] Schegoleva, T.V.: Ageing Mechanism of Alloy Al-Mg-Si, Phys. Metals Metall., Vol. 25(1968), 56-64.
[19] Jacobs, M.H.: Structure of Metastable Precipitates Formed During Aging of an Al-Mg-Si Alloy, Phil. Mag., Vol. 26(1972), 1-13.
[20] Friedel, J.: Dislocations, Pergamon Press, Oxford, 1964, p.329.